

SCOURING AND LOADING OF IDEALIZED BEACHFRONT BUILDING DURING OVERLAND FLOODING

Erdinc Sogut, Stony Brook University, erdinc.sogut@stonybrook.edu
 Ali Farhadzadeh, Stony Brook University, ali.farhadzadeh@stonybrook.edu

The coastlines of the United States are susceptible to tsunamis, windstorms, and other types of flooding hazards. In the past few years, extreme events such as Hurricane Katrina and Hurricane Sandy resulted in the loss of lives and properties, costing the nation billions of dollars (The Office for Coastal Management, 2019). Despite the elevated risk of extreme coastal events, the population in coastal communities has been steadily increasing (Nicholls and Small, 2002; NOAA, 2013). To develop resilient coastal communities, buildings and infrastructures must be designed and constructed such that they are able to withstand extreme flooding. Achieving such an objective necessitates understanding and prediction of flood-induced damages to structures and infrastructures in coastal areas. The existing literature mainly focuses on the current-induced and wave-induced scouring around slender structures. However, structures having dimensions on the scale of incident wave lengths cannot be treated as slender structures. Few studies concentrated on the scour and local hydrodynamics of large bodies, mainly large cylindrical structures (e.g. Katsui, Toue, and others 1993; Sumer and Fredsøe 2001; Toue, Katsui, and Nadaoka 1993).

The main objective of the present study is to investigate the morphodynamics of flooding around near-coast structures. Experimental work has been undertaken to characterize the initiation and development of scour around an idealized building on an erodible berm, during the interaction of a solitary wave with the structure.

METHODOLOGY

A series of flume experiments were carried out for an idealized building with a square cross-section configured in two different layouts (side and center) and exposed to various wave and water level conditions. The experiments were executed at the Coastal and Hydraulic Research Laboratory (CHERL) of Stony Brook University (Fig.1).

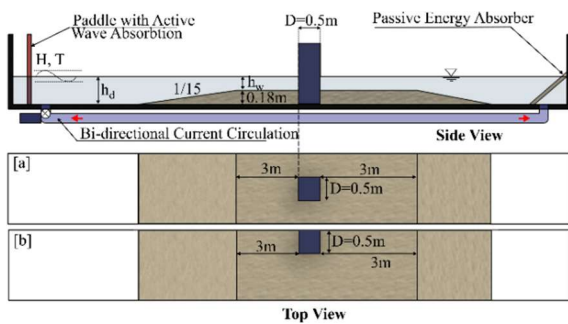


Figure 1 - Top panel shows the cross-sectional view of experimental setup. Panels [a] and [b] show two different layouts with the structure on the side, and center of the channel, respectively. (Not to scale)

The experimental conditions are summarized in Table 1 in which the variables h_d and h_w are water depths in front of the wave paddle and on the beach berm, respectively; H and T are the wave height, and period in front of the wave paddle, respectively; U_m represents the maximum undisturbed near-bottom flow velocity, measured at ~ 2 mm above the sand layer; $KC = U_m T / D$ is the Keulegan-Carpenter number, and D is the structure width.

Table 1 - Characteristics of solitary wave, water level and corresponding near bed velocities

H [m]	L [m]	h_d [m]	h_w [m]	T [s]	U_m [m/s]	D [m]	KC [-]
0.10	7.63	0.480	0.300	3.20	0.491	0.50	3.14
0.75	6.83	0.405	0.225	3.15	0.406	0.50	2.55
0.05	6.15	0.330	0.150	3.19	0.294	0.50	1.87

The structures and the corresponding flows were selected to represent $\lambda=1:40$ length scale according to the Froude similitude.

The free surface elevations were measured at various locations along the flume and around the structures with Edinburgh Designs WG8USB resistive wave gauges (WG) with a sampling capacity of 128 Hz. Undisturbed near bottom velocities (U_m) were recorded before placing the structure on the berm, using a Vectrino Profiler with 25Hz sampling frequency. On the other hand, the velocity field during the test was measured using three Nortek Vectrino Acoustic Doppler Velocimeters (ADV) placed at one-third the still water depth above the berm with a sampling rate of 25 Hz.

The bed was scanned with a HR-Wallingford's HRBP-1070 bed profiler system, equipped with a traverser system for adjusting the position of the profiler in the two or three-dimension setting, before and after each test. Before each test, the surface of the berm was leveled at 0.18m above the flume bottom, the water level gradually rose to the target level and the profiler was calibrated to eliminate potential reading error caused by lab temperature variations. A total length of $4.5D$ of the berm, $2D$ upstream and $2D$ downstream of the structure, was scanned by the profiler in each test. The maneuvering restrictions of the probe created a blind zone of ~ 2 cm around the structure. The bed profile in these zones were manually measured after each test.

RESULTS AND DISCUSSIONS

Figure 2 shows the plan view of the bed elevation variation (S) with respect to the initial bed, and the diameter of the footprint of the scour holes (R_{ave}), both normalized by the structure dimension (D). The scour holes are observed to form around the sharp edges both on the seaside and leeside of the structure in both layouts (Fig. 2). Although the scour hole is deeper on the seaside of the structure, the diameter of the footprint of the scour hole is significantly larger on the leeside. The wake vortices whose trajectories are marked with green spiral curves (Fig. 2) are the driving mechanism in the formation of the scour around this non-slender structure. The wake vortices, discussed by the authors (Sogut et al., 2020, 2019), tend to entrain and transport suspended sediment along their trajectories until they dissipate. Furthermore, it is observed that both depth and diameter of the scour holes significantly depend on the structure layout. Although a deeper scour hole is formed when the structure is positioned on the side, symmetric but relatively shallower scour holes are formed when the structure is positioned in the center.

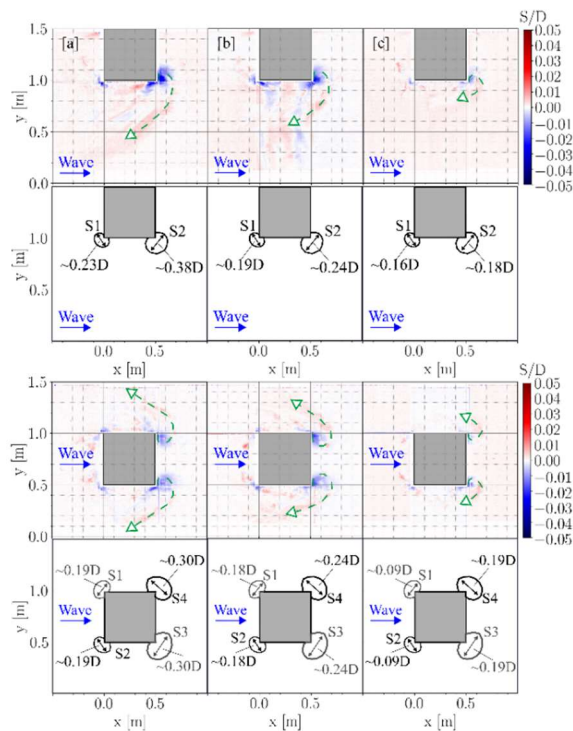


Figure 2 - Plan views of non-equilibrium scour by solitary wave for two different layouts. Panels [a], [b] and [c] corresponds to $H=0.1\text{m}$, 0.75m and 0.05m , respectively. Gray squares represent the structures.

The variations of the maximum S/D , R_{ave}/D , and V_{ave}/V_D with respect to KC are shown in Figure 3. The figure demonstrates that the maximum depth, width, and volume of the scour hole increase more rapidly with KC when the structure is positioned on the side.

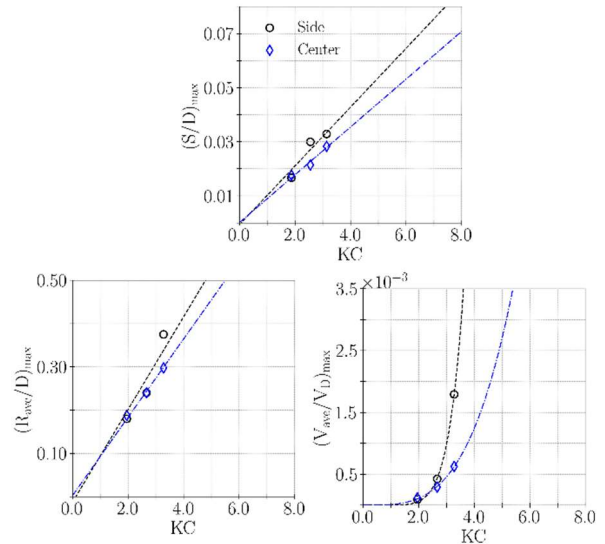


Figure 3 - Variations of maxima of S/D , R_{ave}/D and V_{ave}/V_D with respect to KC . V_D is the characteristic volume which product of cross-sectional area of structure and unit height.

REFERENCES

- Katsui, H., Toue, T., others, 1993. Methodology of estimation of scouring around large-scale offshore structures, in: The Third International Offshore and Polar Engineering Conference.
- Nicholls, R.J., Small, C., 2002. Improved estimates of coastal population and exposure to Hazards released. Eos (Washington, DC). <https://doi.org/10.1029/2002EO000216>
- NOAA, 2013. National coastal population report: Population trends from 1970 to 2010. NOAA State Coast Rep. Ser.
- Sogut, E., Sogut, D.V., Farhadzadeh, A., 2019. Effects of building arrangement on flow and pressure fields generated by a solitary wave interacting with developed coasts. *Adv. Water Resour.* 134. <https://doi.org/10.1016/j.advwatres.2019.103450>
- Sogut, E., Sogut Velioglu, D., Farhadzadeh, A., 2020. Overland Wave Propagation and Load Distribution among Arrays of Elevated Beachfront Structures. *J. Waterw. Port, Coastal, Ocean Eng.* 146, 04020016. [https://doi.org/10.1061/\(ASCE\)WW.1943-5460.0000579](https://doi.org/10.1061/(ASCE)WW.1943-5460.0000579)
- Sumer, B.M., Fredsøe, J., 2001. Wave scour around a large vertical circular cylinder. *J. Waterw. port, coastal, Ocean Eng.* 127, 125-134.
- The Office for Coastal Management, 2019. No Title [WWW Document]. *Natl. Ocean. Atmos. Adm.* URL <https://coast.noaa.gov/states/fast-facts/hurricane-costs.html>
- Toue, T., Katsui, H., Nadaoka, K., 1993. Mechanism of sediment transport around a large circular cylinder, in: *Coastal Engineering 1992*. pp. 2867-2878.